

# Tricritical wings in UGe<sub>2</sub>: A microscopic interpretation

Marcin Abram,<sup>\*</sup> Marcin M. Wysocki,<sup>†</sup> and Józef Spałek<sup>‡</sup>

Marian Smoluchowski Institute of Physics, Jagiellonian University, Łojasiewicza 11, PL-30-348 Kraków, Poland

(Dated: 11 July 2015)

In the present work we analyze the second order transition line that connects the tricritical point and the quantum critical ending point on the temperature–magnetic-field plane in UGe<sub>2</sub>. For the microscopic modeling we employ the Anderson lattice model recently shown to provide a fairly complete description of the full magnetic phase diagram of UGe<sub>2</sub> including all the criticalities. The shape of the so-called tricritical wings, i.e. surfaces of the first-order transitions, previously reported by us to quantitatively agree with the experimental data, is investigated here with respect to the change of the total filling and the Landé factor for  $f$  electrons which can differ from the free electron value. The analysis of the total filling dependence demonstrates sensitivity of our prediction when the respective positions of the critical ending point at the metamagnetic transition and tricritical point are mismatched as compared to the experiment.

PACS numbers: 71.27.+a, 75.30.Kz, 71.10.-w

Keywords: Ferromagnetism, heavy fermions, critical points, UGe<sub>2</sub>

doi:10.1016/j.jmmm.2015.07.017

## I. MOTIVATION AND OVERVIEW

Quantum critical phenomena have captured general attention due to their unique singular properties observed at low temperature ( $T \rightarrow 0$ ) and near the quantum critical point (QCP) which is frequently accompanied by the unconventional superconductivity (SC) [1]. From this perspective,  $f$ -electron compound UGe<sub>2</sub> is a system with phase diagram comprising coexistence of spin-triplet SC and ferromagnetism (FM) [2–6], as well as an abundance of critical points (CP), either of quantum and classical nature [7]. Experimental studies among others have revealed existence of the two characteristic classical CPs in the absence of the field (cf. Fig. 1): (i) the critical ending point (CEP) at 7 K at the metamagnetic transition separating strong (FM2) and weak magnetization (FM1) regions [8–10], and (ii) the tricritical point (TCP) at the FM to paramagnetic (PM) phase transition located at  $T = 24$  K. Additionally, with the applied magnetic field the second order transition line starting from TCP can be followed to  $T = 0$  where it is expected to terminate in a quantum critical ending point (QCEP) [9, 10]. In effect the magnetic phase boundaries in UGe<sub>2</sub> reflects so-called tricritical wing shape.

Such complex magnetic phase diagram with all the above criticalities, both classical and quantum, is particularly challenging in terms of theoretical modeling. One of the first approaches, based on the single-band model describing tricritical wings, was the work by Belitz, et al. [11]. However, the microscopic description of the magnetic phase diagram with all the CPs including also CEP at the metamagnetic transition, as observed in UGe<sub>2</sub>, has been missing until our recent works [13, 14].

Our analysis is based on the (two-orbital) Anderson

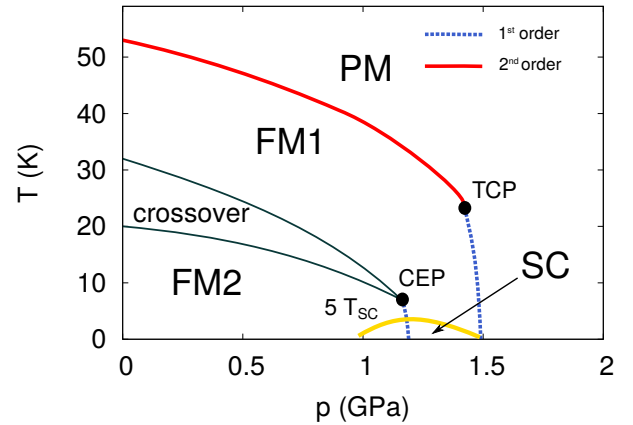


Figure 1. Schematic magnetic phase diagram of UGe<sub>2</sub> on pressure–temperature plane drawn on the basis of the experimental results [9].

lattice model (ALM) [13, 14], often referred to as the periodic Anderson model. Findings for UGe<sub>2</sub>, both from first principle calculations and experiments are: the quasi-two-dimensional character of the Fermi surface [15], a uniaxial anisotropy for magnetization [16], U–U interatomic distance above the so-called Hill limit [1], and the paramagnetic moment per U atom different from that expected for either  $f^3$  or  $f^2$  atomic configurations [2, 17]. We show in the following that all of these findings can be coherently explained within our two-orbital model starting with originally localized  $f$ -states and subsequently being strongly hybridized with the conduction ( $c$ ) band states on a two dimensional lattice and with the applied magnetic field accounted for by the Zeeman term only.

Ferromagnetic order in our model arises from effect of competing hybridization and the  $f$ – $f$  interatomic Coulomb repulsion. The emergence of two distinct ferromagnetic phases is in our model driven by the changing topology of the Fermi surface [18–21] which in turn is

<sup>\*</sup> marcin.abram@uj.edu.pl

<sup>†</sup> marcin.wysocki@uj.edu.pl

<sup>‡</sup> ufspalek@if.uj.edu.pl

induced by a relative motion of hybridized and spin split subbands with the increasing  $f$ - $c$  hybridization. The results obtained from such picture [13] qualitatively agree with the majority of UGe<sub>2</sub> magnetic and electronic properties, as seen in neutron scattering [17], de Haas-van Alphen oscillations [22, 23], and magnetization measurements [8]. Also, a semi-metallic character of the weak FM1 phase is supported by the band-structure calculations [24]. A similar idea concerning the emergence of two distinct FM phases in UGe<sub>2</sub> was also obtained earlier within the phenomenological picture based on the Stoner theory incorporating a two-peak structure of the density of states in a single band [25]. In brief, our microscopic model extended to the case of  $T > 0$  [14] describes well emergence of all CPs on the magnetic phase diagram of UGe<sub>2</sub> [8–10] in the semiquantitative manner [14]. Here we compare in detail our results with the experimental data, namely predicted second order transition line joining the TCP with the corresponding QCEP. In particular, we determine the influence of the following factors: (i) the total band filling  $n$ , and (ii) the value of the Landé factor  $g_f$  for  $f$  states, on the position of this second-order line. The influence of factor (i) has the following importance. For exemplary filling  $n = 1.6$  we have shown [14] that the relative position of the TCP and CEP (cf. Fig.1) is the same as that seen in the experiments [9, 10]. The important question is whether such a mutual alignment of those two critical points is necessary to achieve a good fit and to what extent the proper curvature of the line joining TCP and QCEP is robust with respect to the selected band filling. The discussion of the dependence on (ii) has its justification in the not fully resolved nature of magnetism in heavy-fermion systems in general and UGe<sub>2</sub> in particular. Although it is assumed and widely accepted to be fully itinerant [2], there is evidence for a partially localized contribution [24, 26]. In such case, the influence of the orbital effects and their coupling to the spin should have an influence on  $g_f$  value.

## II. MODEL AND APPROACH

We begin with the orbitally nondegenerate Anderson-lattice model (ALM) on square lattice and with applied magnetic field accounted for via the Zeeman splitting (i.e., with the effective field is  $h \equiv \frac{1}{2}g\mu_0\mu_B H$ ), so that the starting Hamiltonian is

$$\begin{aligned} \hat{\mathcal{H}}_0 = & \sum_{i,j,\sigma} t_{ij} \hat{c}_{i\sigma}^\dagger \hat{c}_{j\sigma} - \sum_{i,\sigma} \sigma h \hat{n}_{i\sigma}^c \\ & + \sum_{i,\sigma} (\epsilon_f - \frac{g_f}{g} \sigma h) \hat{n}_{i\sigma}^f + U \sum_i \hat{n}_{i\uparrow}^f \hat{n}_{i\downarrow}^f \\ & + V \sum_{i,\sigma} (\hat{f}_{i\sigma}^\dagger \hat{c}_{i\sigma} + \hat{c}_{i\sigma}^\dagger \hat{f}_{i\sigma}), \end{aligned} \quad (1)$$

where the onsite hybridization is of magnitude  $V < 0$  and the Landé factor for  $f$  electrons is  $g_f$  (the free electron value is  $g = 2$ ). The model describes a two-orbital system

with the conduction ( $c$ ) band arising from the nearest ( $t$ ) and the second-nearest ( $t'$ ) neighbor hoppings, and the strong  $f$ - $f$  Coulomb interaction is of magnitude  $U$ . If it is not stated otherwise, we set  $t' = 0.25|t|$ ,  $U = 5|t|$ ,  $\epsilon_f = -3|t|$ ,  $g_f = g = 2$ , and  $n \equiv \sum_\sigma \langle \hat{n}_{i\sigma}^c + \hat{n}_{i\sigma}^f \rangle = 1.6$ .

We also add to the Hamiltonian (1) the usual term with the chemical potential  $\mu$ , i.e.,

$$\hat{\mathcal{H}} \equiv \hat{\mathcal{H}}_0 - \mu \sum_{i,\sigma} (\hat{n}_{i\sigma}^c + \hat{n}_{i\sigma}^f). \quad (2)$$

The model is solved here by means of *statistically consistent Gutzwiller approximation* (SGA) [27–29]. The method was successfully applied to the number of problems [30, 31]. It is characterized with the physical transparency and flexibility, that it could be also incorporated into other methods such as EDABI [32, 33].

We introduce the Gutzwiller projection acting onto uncorrelated wave function  $|\psi_0\rangle$  in the following manner

$$|\psi_G\rangle = \prod_i P_{G;i} |\psi_0\rangle, \quad (3)$$

where  $|\psi_G\rangle$  is the wave function of the correlated ground state. In effect, we map many-particle correlated Hamiltonian (1) onto an effective single-particle Hamiltonian  $\hat{\mathcal{H}}_{SGA}$  acting on uncorrelated wave function  $|\psi_0\rangle$ , that, after taking the space Fourier transform, is as follows

$$\begin{aligned} \hat{\mathcal{H}}_{SGA} \equiv & \hat{\Psi}_{\mathbf{k}\sigma}^\dagger \begin{pmatrix} \epsilon_{\mathbf{k}}^c - \sigma h - \mu & \sqrt{q_\sigma} V \\ \sqrt{q_\sigma} V & \epsilon_f - \sigma \frac{g_f}{g} h - \mu \end{pmatrix} \hat{\Psi}_{\mathbf{k}\sigma} \\ & - \lambda_n^f \left( \sum_{\mathbf{k},\sigma} \hat{n}_{\mathbf{k}\sigma}^f - \Lambda n_f \right) - \lambda_m^f \left( \sum_{\mathbf{k},\sigma} \sigma \hat{n}_{\mathbf{k}\sigma}^f - \Lambda m_f \right) \\ & + \Lambda U d^2 \end{aligned} \quad (4)$$

where  $\hat{\Psi}_{\mathbf{k}\sigma}^\dagger \equiv (\hat{c}_{\mathbf{k},\sigma}^\dagger, \hat{f}_{\mathbf{k},\sigma}^\dagger)$ ,  $\Lambda$  is the number of the system sites,  $q_\sigma$  is the hybridization narrowing factor, and  $d^2 \equiv \langle \hat{n}_{i\uparrow}^f \hat{n}_{i\downarrow}^f \rangle_0$  [31]. Necessary constraints for the  $f$  electron number and their magnetic moment [29] are incorporated by means of the Lagrange multipliers  $\lambda_n^f$  and  $\lambda_m^f$ , respectively. Hamiltonian (4) can be straightforwardly diagonalized with the resulting four eigenvalues  $\{E_{\mathbf{k}\sigma}^b\}$  labeled with the spin ( $\sigma = \pm 1$ ) and hybridized-band ( $b = \pm 1$ ) indices. For  $T > 0$  we construct a generalized Landau grand-potential functional according to

$$\begin{aligned} \frac{\mathcal{F}}{\Lambda} = & - \frac{1}{\Lambda\beta} \sum_{\mathbf{k}\sigma b} \ln[1 + e^{-\beta E_{\mathbf{k}\sigma}^b}] \\ & + (\lambda_n^f n_f + \lambda_m^f m_f + U d^2), \end{aligned} \quad (5)$$

which is next minimized with respect to the set of following parameters assembled to a vector,  $\vec{\lambda} \equiv \{d, n_f, m_f, \lambda_n^f, \lambda_m^f\}$ . Additionally, we adjust self-consistently the chemical potential from the condition of fixing the total number of electrons,  $n = 1/\Lambda \sum_{\mathbf{k}b\sigma} f(E_{\mathbf{k}\sigma}^b)$ , where  $f(E)$  is the Fermi-Dirac function. Finally the ground state energy is defined by,

$$E_G = \mathcal{F}|_0 + \mu N, \quad (6)$$

where  $\mathcal{F}|_0$  means that the value of  $\mathcal{F}$  is taken at minimum for the parameters  $\bar{\lambda}$ .

### III. RESULTS AND DISCUSSION

We start our analysis with the discussion on the proper assignment of the physical units to the microscopic parameters provided so far in dimensionless units (i.e. scaled by  $|t|$ ) to make the quantitative comparison with the observed  $\text{UGe}_2$  characteristics. To do so, we have adjusted them [14] by matching the relative positions of the two classical CPs: TCP and CEP at the ferromagnetic transition, as well as attributing the experimentally measured critical temperatures. Matching the results in physical units by fixing the position of two critical points we would call a *strong fitting*, whereas by fixing the position of just a single of them a *weak fitting*.

In our previous works [13, 14] we have found that for the total filling  $n = 1.6$  we could coherently and quantitatively describe the  $\text{UGe}_2$  phase diagram. Although, there is no direct experimental evidence in  $\text{UGe}_2$  for choosing this particular filling, we have first matched for chosen  $n$  TCP and CEP temperatures according to the experiment [14] – strong fitting condition, and second, we have verified our prediction obtaining agreement of the second-order transition line joining TCP with QCEP [10] with that measured. Additionally, the comparison has provided among others the estimate of the QCEP appearance about 30 T, i.e., higher than that suggested in Ref. [10] which is 18 T.

A natural question arises if this test is sensitive to the choice of  $n$ . We show in Fig. 2 that the second-order transition line joining TCP and QCEP determined for a slightly different total filling than  $n = 1.6$  deviates significantly from the trend of the experimental data [10]. Hence indeed, the comparison is very sensitive to the choice of  $n$ . Thus, together with equally sensitive adjustment of  $T_{TCP}$  and  $T_{CEP}$  with respect to the choice of  $n$  [14], it is unlikely that our excellent agreement for the single value of parameter  $n$  is fortuitous.

For the sake of completeness and reference to other related works we include in Fig. 2 the (dashed) curve predicted by the one of the most successful approaches describing the general tricritical behavior in itinerant magnetic systems [11, 12]. In that procedure, the necessary inputs are the positions of the two CPs, namely TCP and QCEP, leading in fact to the *strong fitting*, but with different pair of CPs. However, such fitting can be associated with an error as the position of the QCEP, in contrast to TCP and CEP, is not experimentally determined but only extrapolated to 18 T, following Ref. [10]. Note that this condition in our modeling is satisfied for the total filling around  $n \simeq 1.55$  (cf. Fig. 2) if we take the extrapolated value of the critical field. In this case, the comparison with results for  $\text{UGe}_2$  [10] is worse than e.g. for  $n = 1.6$  and the temperature of the CEP is much lower than that determined in experiments [8].

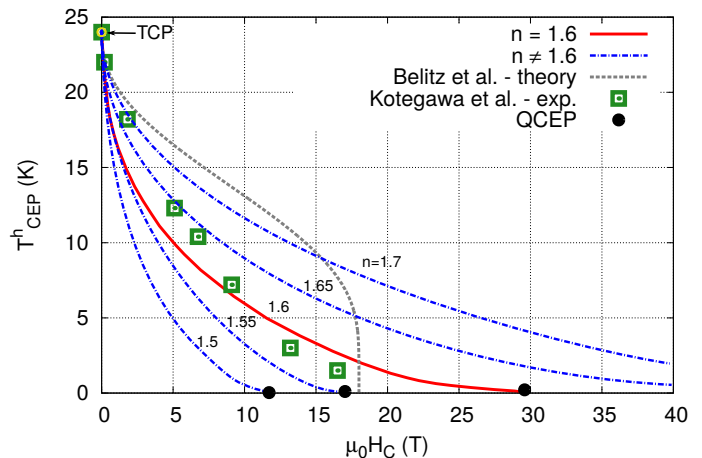


Figure 2. The second-order transition line joining TCP and QCEP for selected values of total filling,  $n$ . Solid, red curve is replotted from the results reported in Ref. [14]. Experimental points are extracted from pictures in Ref. [10]. Grey, dashed curve predicted by the theory formulated by Belitz, et al. [11] is shown for comparison (see main text).

It is worth mentioning that the model employed by us belongs to the class discussed earlier by Kirkpatrick and Belitz [12] to reflect the generic tricriticality in the case of metallic magnets. Namely, systems in which the conduction electrons are not a source of the magnetism themselves, but are couple to the magnetically ordered localized electrons in a second band. The origin of the first-order transition at low temperature described within the mean-field theory developed in the Refs. [11, 12] is based on the effect of the soft fermionic modes coupled to the magnetization fluctuations, and thus differs from our approach. Here the mechanism for ferromagnetism is due to the coupling of the conduction electrons with localized  $f$  states by hybridizing with them and competing with the  $f$ - $f$  Coulomb interaction. This competition in the Stoner-like manner induces phase transitions associated with the abrupt changes of the Fermi surface topology.

The simplest verification of our analysis can be carried out by means of chemical alloying, i.e., by changing the electron concentration in the system. However, the lack of known isostructural compounds to  $\text{UGe}_2$  may be an apparent obstacle for such test. Though, the determination of the tail of the 2nd order line joining TCP and QCEP for the field larger than 16 T should provide an insight on the issue whether our model correctly predicts the appearance of QCEP around 30 T [14].

If our model is to be used to understand the magnetism of other ferromagnetic superconductors:  $\text{URhGe}$  [34] and  $\text{UCoGe}$  [35], it would provide a perfect testing ground of our model as those compounds have been frequently studied by means of the chemical substitution [1, 3–6].

Finally, we provide a brief analysis of the impact of the Landé factor value for  $f$  electrons,  $g_f$ , i.e., in the situation when the  $z$  component of the total spin of the

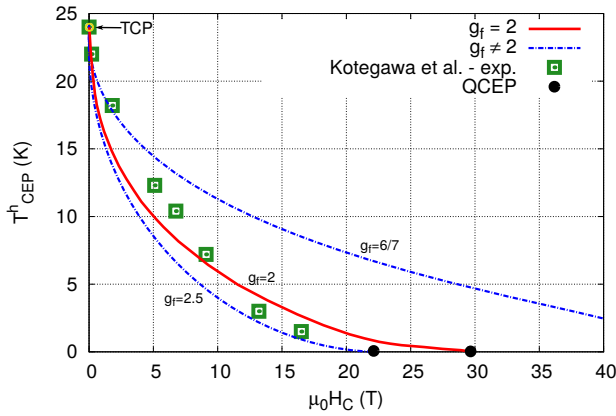


Figure 3. The second-order transition line joining TCP and QCEP for selected values of Landé factor for  $f$  electrons,  $g_f$ . Solid curve for  $g_f = 2$  is replotted from the results reported in Ref. [14]. Experimental points are extracted from Ref. [10].

system does not commute with Hamiltonian. In Fig. 3 we present the curves for three different values of  $g_f$ . The curve for  $g_f = 2$ , is plotted as the reference curve and is based on the results of Ref. [14]. Value of  $g_f$  is not known for  $\text{UGe}_2$  and generally, for complex compounds it has a tensor character which depends on the magnitude of the spin-orbit coupling. For that reason we restrict our discussion to the comparison when  $g_f$  is equal to the free electron value  $g_f = 2$ , and subsequently when it is lower and higher (cf. Fig.3) [36]. Specifically, the lower value of Landé factor  $g_f = 6/7$  is motivated by that for the Ce-based compounds, where it can be derived for the spin  $S = 1/2$  and angular momentum  $L = 3$ , oriented antiparallel and where, strictly speaking, our model is also generally valid, as long as we do not account for the orbital degeneracy of  $f$  states of the uranium-based materials. As presented in Fig. 3, it seems that any value of  $g$  factor for  $f$  states which deviates considerably from the free-electron value, provides much worse agreement with experimental data [10]. In conclusion, due to predominantly itinerant nature of  $f$  electrons in  $\text{UGe}_2$  [26], it is very likely that any crystal-field derived multiplet structure is washed out and hence the value  $g_f \approx 2$  should be regarded as realistic value. Nevertheless, the problem of double localized-itinerant nature of  $f$ -electrons [24, 26] may arise as the system evolves with the increasing temperature, in comparison to the pressure evolution at low temperature studied in detail here.

#### IV. OUTLOOK

In the present work we have employed the Anderson lattice model [13, 14] to provide a fairly complete descrip-

tion of the magnetic phase diagram ( $p$ - $T$ - $h$  profiles) of  $\text{UGe}_2$  including all the criticalities for this compound. In particular, we study the effect of the choice of the total filling on the quality of the fit, based on our model, to the experimental data [10] concerning the second-order transition line joining the critical points TCP and QCEP. We have found that our prediction is very sensitive to the change of  $n$ , which leads also to a mismatch of critical temperatures of TCP and CEP at the metamagnetic transition as compared to the experiment. We infer from this result that our excellent agreement for the single value of  $n$  is unlikely fortuitous. We have also analyzed the effect of the Landé factor  $g_f$  value for  $f$  electrons. In this case, any sizable deviation from the free electron value  $g_f = 2$  shifts the theoretical curves away from the experimental points. Thus treating  $f$  electrons as truly itinerant electrons in  $\text{UGe}_2$  seems to be fully justified.

Our final remark addresses the problem of the spin-triplet superconductivity (SC) origin occurring in  $\text{UGe}_2$  [1, 2]. We have predicted in our previous work [14] the appearance of QCP in the vicinity of the SC dome. It has been proposed that that CEP (cf. Fig. 1) at the metamagnetic phase boundary can be followed down to the  $T = 0$  by changing both the electron concentration and the hybridization magnitude  $|V|$  (cf. Fig. 4). The proposed quantum critical point is of Lifshitz type as it separates states with two distinct Fermi-surface topologies. Quantum critical fluctuations or the residual  $f$ - $f$  Hund's rule interaction (neglected here) can become the possible source of the spin-triplet superconductivity [37–41]. A detailed and quantitative discussion of the pairing requires a separate analysis.

*Acknowledgements.* The work was supported by the National Science Centre (NCN) under the Grant MAE-STRO, No. DEC-2012/04/A/ST3/00342.

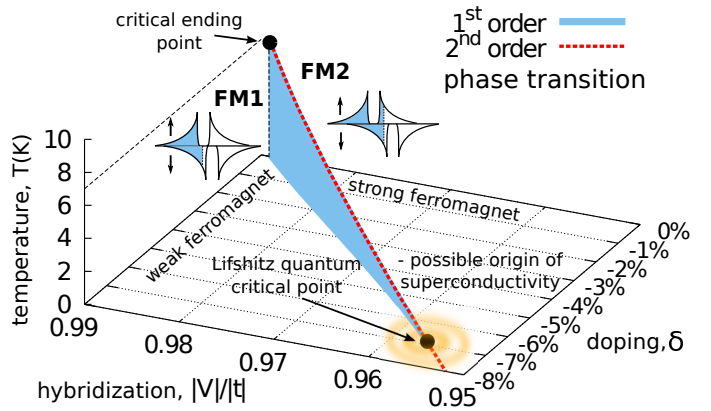


Figure 4. Evolution of the critical temperature of CEP towards Lifshitz QCP driven by changing total filling,  $n$  and hybridization,  $V$  reproduced after [14].

- 
- [1] C. Pfleiderer, *Rev. Mod. Phys.* **81**, 1551 (2009).
- [2] S. S. Saxena, P. Agarwal, K. Ahilan, F. M. Grosche, R. K. W. Haselwimmer, M. J. Steiner, E. Pugh, I. R. Walker, S. R. Julian, P. Monthoux, G. G. Lonzarich, A. Huxley, I. Sheikin, D. Braithwaite, and J. Flouquet, *Nature* **406**, 587 (2000).
- [3] D. Aoki and J. Flouquet, *J. Phys. Soc. Jpn.* **81**, 011003 (2012).
- [4] D. Aoki, A. Gourgout, A. Pourret, G. Bastien, G. Knebel, and J. Flouquet, *C. R. Physique* **15**, 630 (2014).
- [5] D. Aoki and J. Flouquet, *J. Phys. Soc. Jpn.* **83**, 051011 (2014).
- [6] A. D. Huxley, *Physica C* **514**, 368 (2015).
- [7] Coexistence of FM and SC was observed for the first time by A. Kolodziejczyk for the weak itinerant ferromagnets  $\text{Y}_9\text{Co}_7$  [42–44]. However, SC was found there to be of spin-singlet nature and strongly competing with FM, in contrast to the  $\text{UGe}_2$  case, where it is of the spin-triplet character and its coexistence with FM seems to be strongly cooperative as e.g. both phases disappear at the same pressure.
- [8] C. Pfleiderer and A. D. Huxley, *Phys. Rev. Lett.* **89**, 147005 (2002).
- [9] V. Taufour, D. Aoki, G. Knebel, and J. Flouquet, *Phys. Rev. Lett.* **105**, 217201 (2010).
- [10] H. Kotegawa, V. Taufour, D. Aoki, G. Knebel, and J. Flouquet, *J. Phys. Soc. Jpn.* **80**, 083703 (2011).
- [11] D. Belitz, T. R. Kirkpatrick, and J. Rollbühler, *Phys. Rev. Lett.* **94**, 247205 (2005).
- [12] T. R. Kirkpatrick, and D. Belitz, *Phys. Rev. B* **85**, 134451 (2012).
- [13] M. M. Wysokiński, M. Abram, and J. Spalek, *Phys. Rev. B* **90**, 081114(R) (2014).
- [14] M. M. Wysokiński, M. Abram, and J. Spalek, *Phys. Rev. B* **91**, 081108(R) (2015).
- [15] A. B. Shick and W. E. Pickett, *Phys. Rev. Lett.* **86**, 300 (2001).
- [16] A. Huxley, I. Sheikin, E. Ressouche, N. Kernavanois, D. Braithwaite, R. Calemczuk, and J. Flouquet, *Phys. Rev. B* **63**, 144519 (2001).
- [17] N. Kernavanois, B. Grenier, A. Huxley, E. Ressouche, J. P. Sanchez, and J. Flouquet, *Phys. Rev. B* **64**, 174509 (2001).
- [18] R. Doradziński and J. Spalek, *Phys. Rev. B* **56**, R14239 (1997).
- [19] R. Doradziński and J. Spalek, *Phys. Rev. B* **58**, 3293 (1998).
- [20] O. Howczak, J. Kaczmarczyk, and J. Spalek, *Phys. Stat. Solidi (b)* **250**, 609 (2013).
- [21] K. Kubo, *Phys. Rev. B* **87**, 195127 (2013).
- [22] T. Terashima, T. Matsumoto, C. Terakura, S. Uji, N. Kimura, M. Endo, T. Komatsubara, and H. Aoki, *Phys. Rev. Lett.* **87**, 166401 (2001).
- [23] R. Settai, M. Nakashima, S. Araki, Y. Haga, T. C. Kobayashi, N. Tateiwa, H. Yamagami, and Y. Onuki, *J. Phys: Condens. Matter* **14**, L29 (2002).
- [24] M. Samsel-Czekala, M. Werwiński, A. Szajek, G. Chełkowska, and R. Troć, *Intermetallics* **19**, 1411 (2011).
- [25] K. G. Sandeman, G. G. Lonzarich, and A. J. Schofield, *Phys. Rev. Lett.* **90**, 167005 (2003).
- [26] R. Troć, Z. Gajek, and A. Pikul, *Phys. Rev. B* **86**, 224403 (2012).
- [27] T. M. Rice and K. Ueda, *Phys. Rev. Lett.* **55**, 995 (1985).
- [28] P. Fazekas and B. H. Brandow, *Phys. Scr.* **36**, 809 (1987).
- [29] J. Jędrak, J. Kaczmarczyk, and J. Spalek, arXiv:1008.0021 .
- [30] M. Abram, J. Kaczmarczyk, J. Jędrak, and J. Spalek, *Phys. Rev. B* **88**, 094502 (2013).
- [31] M. M. Wysokiński and J. Spalek, *J. Phys.: Condens. Matter* **26**, 055601 (2014).
- [32] A. P. Kądziaława, J. Spalek, J. Kurzyk, and W. Wójcik, *The European Physical Journal B* **86**, 252 (2013).
- [33] A. P. Kądziaława, *Acta Phys. Pol. A* **126**, A58 (2014).
- [34] D. Aoki, A. Huxley, E. Ressouche, D. Braithwaite, J. Flouquet, J.-P. Brison, E. Lhotel, and C. Paulsen, *Nature* **413**, 613 (2001).
- [35] N. T. Huy, A. Gasparini, D. E. de Nijs, Y. Huang, J. C. P. Klaasse, T. Gortenmulder, A. de Visser, A. Hamann, T. Görlach, and H. v. Löhneysen, *Phys. Rev. Lett.* **99**, 067006 (2007).
- [36] P. Quinet and E. Biémont, *Atomic Data and Nuclear Data Tables* **87**, 207 (2004).
- [37] M. Zegrodnik and J. Spalek, *Phys. Rev. B* **86**, 014505 (2012).
- [38] M. Zegrodnik, J. Spalek, and J. Bünnemann, *New J. Phys.* **15**, 073050 (2013).
- [39] J. Spalek and M. Zegrodnik, *J. Phys.: Condens. Matter* **25**, 435601 (2013).
- [40] M. Zegrodnik, J. Bünnemann, and J. Spalek, *New J. Phys.* **16**, 033001 (2014).
- [41] J. Spalek, *Phys. Rev. B* **63**, 104513 (2001).
- [42] A. Kolodziejczyk, B. V. Sarkissian, and B. R. Coles, *J. Phys. F* **10**, L333 (1980).
- [43] A. Kolodziejczyk, *Physica B* **130**, 189 (1985).
- [44] K. Rogacki, A. Kolodziejczyk, L. Bochenek, and T. Cichorek, *Phil. Mag.* **95**, 503 (2015).